Debridement 2.0 – A semi-automated robotic system challenges traditional assumptions

Cornelia Häusler, Felix Fussenegger, Andreas Hahnekamp, Christoph Kment, Johannes Schnur, Alexander Unger, Herbert Weißenböck

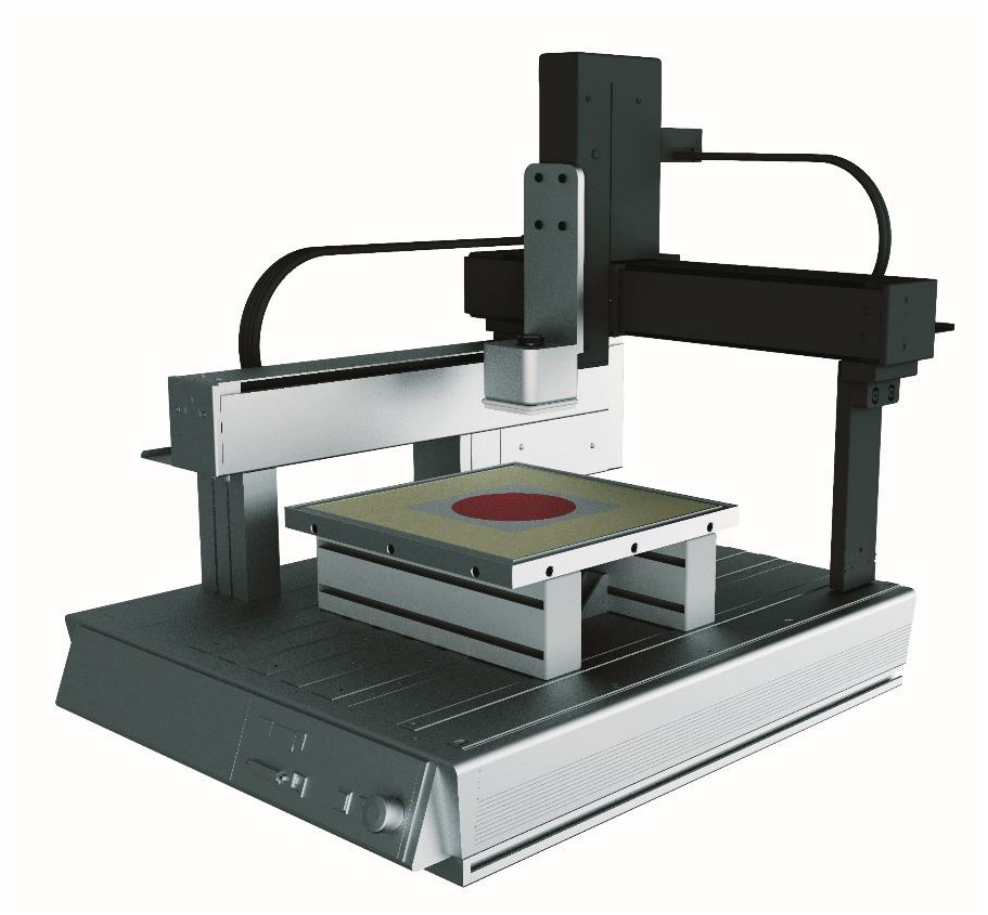

Abstract

Objective: Appropriate wound debridement plays a key role in wound management and healing. In this study, we developed and evaluated a novel clinic-related *in-vitro* test system for detailed analysis of mechanical wound debridement procedures. The acquired knowledge can be used to improve existing products and processes, or to develop completely new ones.

Approach: The application-oriented *in-vitro* simulation system for wound debridement comprises debridement process tracking and a robotic debridement simulation device together with artificial wounds**.**

Results: Wound debridement movements, number of movement cycles, velocities as well as contact forces of medical experts were recorded in real-time by the debridement tracking device and reproduced with the robotic system. Mechanical debridement products were tested on developed artificial wounds and evaluated regarding certain parameters such as efficacy of wound debridement and product uptake. Reproducibility and statistically significance of obtained *in-vitro* results verified the functionality and suitability of our system.

Innovation: The system represents an innovative and objective tool for a variety of product and process analysis in an application-oriented test arrangement, and challenges traditional assumptions that exclude real-time individuality. Obtained data can be used for optimization of wound debridement strategies.

Conclusion: The semi-automated robotic system allows an effective learning process, from *real-time* tracking to *in-vitro* testing and finally back to real-time application. This new approach provides a strong link between *in-vitro* analysis and clinical applications.

Introduction

Wound debridement plays a key role in the management and healing of wounds. The debridement process involves the removal of contaminated, adherent, or necrotic tissue impeding the natural healing process of the wound [1]. A lack of appropriate wound treatment may result in inflammation and bacterial colonization [2]. The debridement procedure as well as suitable debridement products must be selected considering the individual wound conditions. The result of debridement is strongly related to product properties combined with application skills and experience of the user.

Due to the high variability of wounds [3], it is a challenge to provide and reproduce defined conditions in order to test wound debridement strategies in a systematic and comparable way. Apart from classical debridement basic products and procedures, the medical personnel usually deploy some preferred products [4] and carries out individual procedure variants. As Gillespie *et al.* (2014) showed in a study, wound management decisions in daily clinical work tend to be practice-based and strongly intuitive [5].

A quite simple form of a semi-automated *in-vitro* test setup to analyze wound debridement performance was published by University Medical Center Jena and Lohmann & Rauscher [6, 7, 8, 9, 10]. This setup consists of a one-dimensional motor-driven device together with an inserted glass plate covered with a protein-containing mixture as wound simulation. It allows the simulation of a simple, linear debridement process with a mechanical debridement product under a defined contact force, realized by using a weight. Further linear debridement test setups were published by Wilkinson *et al. (*2016) [11] and Gafford *et al.* (2016) [12].

A small robot arm for debridement tests, executing simple, two-dimensional patterns on structured plates, was published by Igwebuike and Hoeier Nielsen in 2019 [13]. Another robot arm-based application targeting wound treatment was presented in the publication from Karnam and Asokan (2013) [14]. The proposed system is based on an image processing component that identifies the

location and critical parameters of the wound, and a robotic arm for mechanically treating the wound. Schoeb *et al.* (2018) published a robot-based application of wound debridement simulation, deploying a robot arm with nine degrees of freedom [15]. In 2019, Schlenk *et al.* demonstrated a robotic waterjet system suitable for wound debridement applications [16]. A wound debriding and medicine application robot is also disclosed in patent CN109276801A, published in 2019 [17].

An open issue with these existing systems is the lacking connection between clinical applications and *in-vitro* testing. To solve this problem, we developed a system fulfilling all necessary requirements, including a tracking device to record real-time data, a robotic device for the execution of *in-vitro* debridement simulation as well as a series of artificial wounds.

In this study, we evaluated the suitability of our semi-automated robotic system for detailed analysis of mechanical wound debridement procedures with the aim of both improving already existing products and processes as well as developing completely new ones.

Innovation

Traditional debridement analysis systems exclude the fact of real-time application individuality in the clinic. Our developed system includes tracking and integration of real clinical debridement characteristics (Fig 1), thus providing a strong link to clinical applications. It enables reproducible, valid comparisons of products and processes, opening the possibility to develop target-oriented treatments for different wound conditions. In its entirety, the system could serve as the basis for prospective test standards. Due to the unique combination of real-time procedures and *in-vitro* analysis, the new approach offers great advantages for patients, users, and companies in the field of medical consumables and beyond.

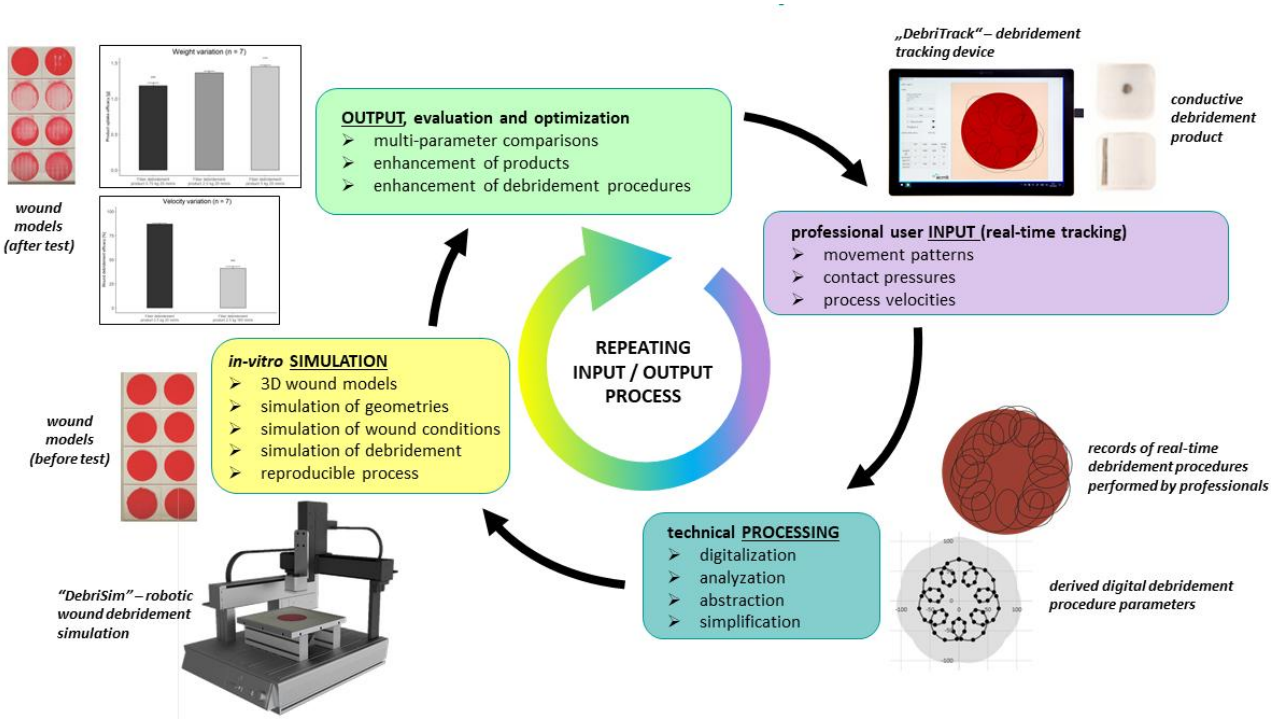

Figure 1. Innovation process. The semi-automatic robot system comprises a repeating input-output process. Inputs are generated by real-time tracking of debridement procedures simulated by wound care professionals. The recorded data are technically processed to feed the debridement parameters into the robot, which reproduces them. After execution of the debridement process by the robot on simulated wounds, the obtained output is evaluated. Clinical wound debridement processes can be optimized based on the acquired knowledge.

Clinical Problem Addressed

Wound debridement processes are characterized by different parameters, such as velocity, movement pattern or contact force. The variability of these parameters during debridement processes leads to a high degree of individuality in real-time applications. In order to apply and combine the parameters as efficiently as possible, it is necessary to simulate the individual real-time parameters within *in-vitro* tests to learn about their mode of action and influence. Furthermore, it is essential to know the functionality of debridement products in detail, to tune their properties and thus achieve maximum efficacy in treatment. Our *in-vitro* test system offers the possibility to simulate defined debridement and wound conditions, thus allowing detailed analysis of mechanical debridement processes and products in a valid, reproducible way.

Material and Methods

The application-oriented robotic wound debridement simulation system consists of the debridement procedure tracking device named "*DebriTrack*" and the robotic debridement simulation device "*DebriSim*". The debridement performance is evaluated on artificial wounds examining parameters such as efficacy of wound debridement and product uptake.

Debridement parameter acquisition with „*DebriTrack*"

To replicate wound debridement processes as closely as possible, relevant parameters are acquired and subsequently transferred to the robot with our developed tracking device *DebriTrack*. The device represents a simplified wound and offers the possibility to measure and display real-time user movement patterns, velocities and contact forces during simulated wound debridement procedures (Fig 2, Mov S1).

Data are recorded, processed, and displayed on a tablet PC (Microsoft Surface Pro 5; Microsoft Corp., US) using a software application created with the LabVIEW™ (National Instruments Corp., US) development environment. Debridement force is measured by four force gauges (TE Connectivity Ltd., CHE) integrated in a sensing platform, which is placed beneath the tablet PC and connected via USB. Debridement products are made locally conductive to record the movement pattern on the capacitive screen of the tablet PC. For this purpose, a conductive mesh (NASAFES®, US) was integrated into the fabric structure (Fig 2). The simplified representation of a wound area, visualized in red, corresponds to the wound models to be inserted into the *DebriSim* robot. *DebriTrack* registers the movements during debridement on the touchscreen and records timestamps, positions, contact pressures and velocities. Afterwards, the captured debridement procedure parameters can be replayed on *DebriTrack* in an itemized form, serving for subsequent visual analysis and comparisons of different

debridement sessions. The tracked debridement data sets can be modified and exported to be used either for execution on *DebriSim* or for external data analysis.

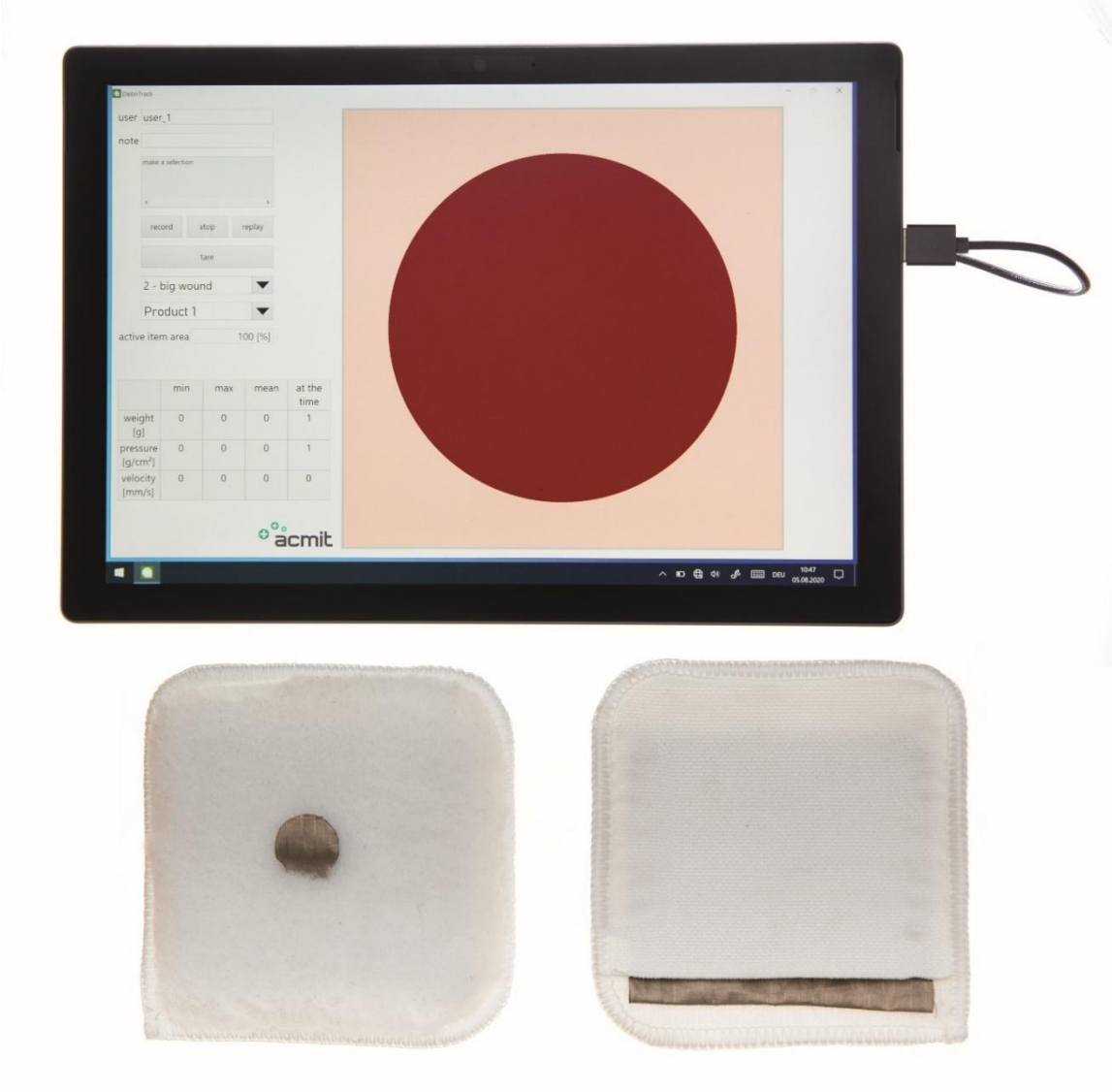

Figure 2. *DebriTrack*. The device includes a force sensing platform (not shown here), a test surface depicting a virtual wound and modified debridement test products, equipped with a conductive mesh (front and back side shown). The force sensing platform and the tablet PC are connected via USB.

Debridement simulation device „*DebriSim*“

The core component of *DebriSim* (Fig 3, Mov S2) is a tabletop robot model IAI TTA-C (IAI Industrieroboter GmbH, GER) that can perform movements along the x-, y- and z-axis. The range of velocity is defined to be 20 – 160 mm/s. The vertical force that can be applied by the robot ranges from 5 to 19 kg (corresponding load). For lower loads (0.75 to 5 kg) a floating mass module was added to the robotic arm. The velocity and load ranges are based on clinical measurements. The robot memory is programmed with a set of movement parameters derived from clinical procedures (e.g., Fig 4 – Fig 6).

The robot is operated by a custom-made control panel. It allows the selection of various pre-programmable debridement patterns, the control of loads and velocities, pattern repetitions as well as program initiation and termination. An implemented top-view digital camera (Canon GX5, Canon Inc., JP) is remotely controlled and automatically documents the debridement progress. In addition, a manual shutter release for the camera is implemented on the control panel to provide individual test documentation. An LED ring light can be used to ensure constant ambient lighting.

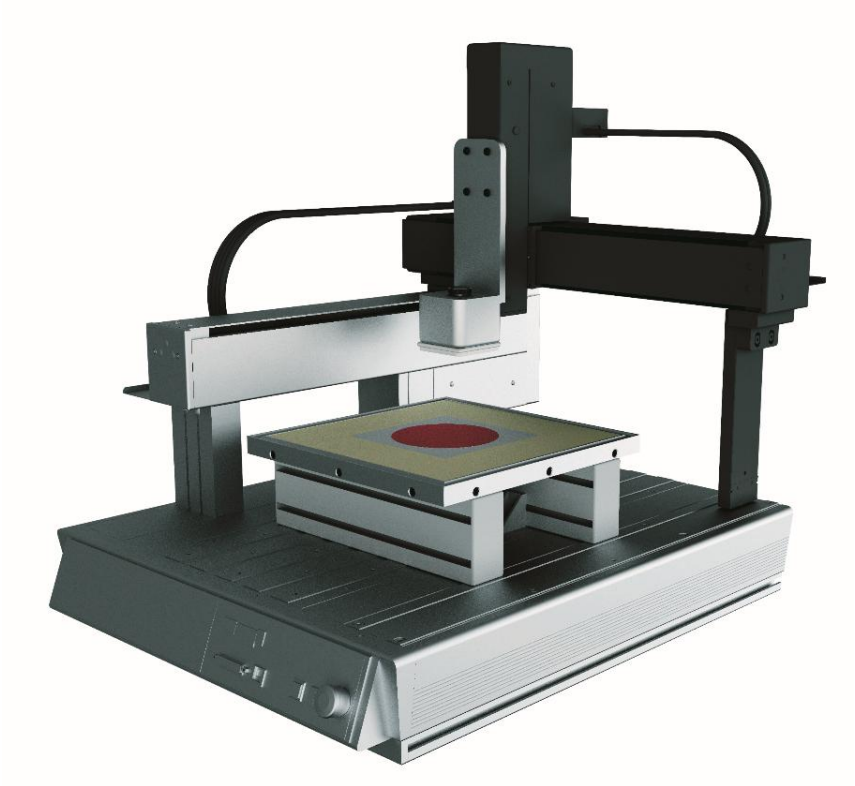

Figure 3. *DebriSim*. Schematic representation of the robot construction with inserted artificial wounds and an attached test sample on the gripper.

Various holders were developed enabling the attachment of different debridement products to the robot arm. The holders differ in their contact surface shape to simulate different product handling techniques. Products are fixed on the holder either by hook tape or by holding clamps. The standard holder is a 3D printed block of 80 x 80 mm size with rounded corners, equipped with hook tape (Velcro®, UK).

Before starting a test procedure, a corresponding artificial wound must be inserted into the robotic system.

Artificial wounds

The wound models consist of an acrylic base plate with a central circular area, structured by a laser cutter (VersaLASER VLS3.50; Universal Laser Systems GmbH, AT), to ensure adequate adhesion of our developed wound fluid or coating simulations.

The size of treated wounds is an important factor for the wound debridement process. Sizes of the simulated wound areas determined in an internal survey among Lohmann & Rauscher customers (2013) reach from wound areas smaller than 25 cm² (19 % of the wounds) to wound areas bigger than 225 cm² (32 % of the wounds), with most wounds (49 %) between these borders.

To simulate different wound sizes, we designed two wound dimensions: models with a plate size of 80 x 80 mm, displaying a circular wound of 60 mm diameter (≙ 28 cm² wound area), and models with a plate size of 150 x 150 mm with a wound diameter of 120 mm (≙ 113 cm² wound area).

Finally, our developed simulations of exudate, fibrin coatings, burns and necroses, which are described in the results chapter, must be applied on the circular wound area. On the small wound models 4 ml of simulation must be applied and on the large wound models 16 ml.

Results

Determination and reproduction of real-time debridement movement patterns

Recording of debridement patterns performed by wound care professionals

Compactness and transportability of the *DebriTrack* enables uncomplicated collection of real-time application data. We recorded a series of wound debridement patterns at the *Leg Ulcer Clinic - Day Hospital, Deeside Community Hospital* in Wales, UK (example shown in Fig 4).

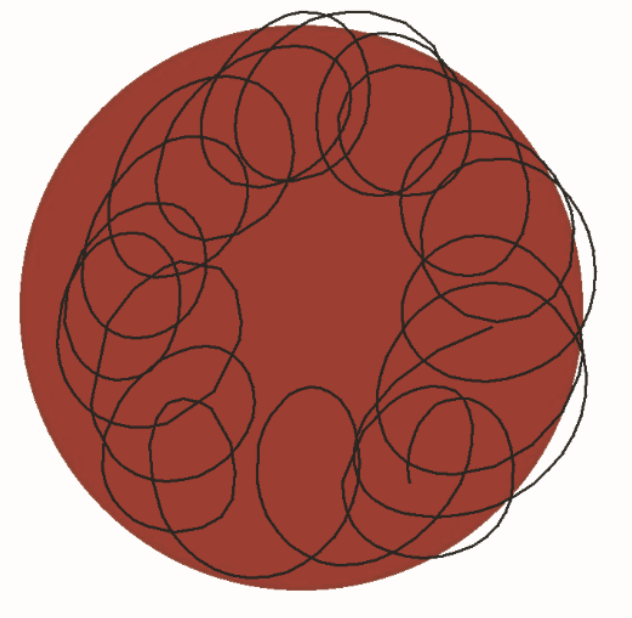

Figure 4. Sample of a hypocycloid movement pattern from a real-time recording created by a medical wound manager. Red circle = wound area, black line = recorded track (center of the debridement product served as contact area)

Mathematical translation to robot compatible data sets

Based on individual working preferences of test persons, we tracked various debridement patterns. The tracked patterns revealed regularities.

An in-depth visual analysis of recorded patterns made it possible to trace them back to a series of simplified mathematical patterns. A frequently observed movement pattern resembled a rosette, or, from a mathematical point of view, hypocycloids (Fig 4). The movement of a point on the rolling circle can be described by the following parametric equations (Fig 5):

$$x(t) = (R-r)\cos\left(\frac{r}{R}t\right) + r_p \cos\left(\left(1-\frac{r}{R}\right)t\right),\ \ y(t) = (R-r)\sin(\frac{r}{R}t) - r_p \sin((1-\frac{r}{R})t) \tag{1}$$

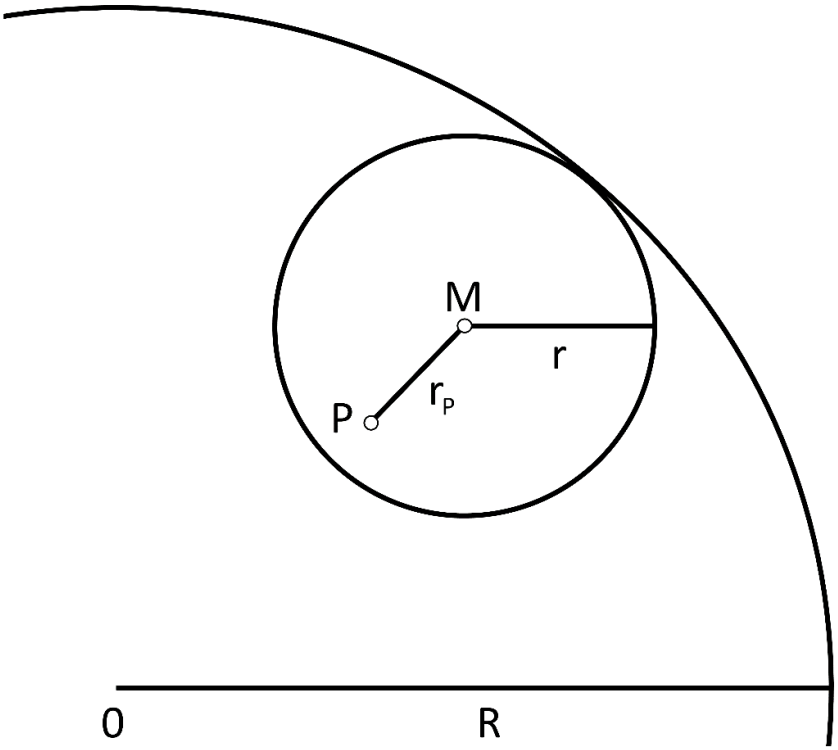

Figure 5. Graphical illustration for the generation of a hypocycloid for point P.

Using these equations discrete points were calculated and loaded into the robot controller memory. Fig 6 shows one of the resulting cycloids:

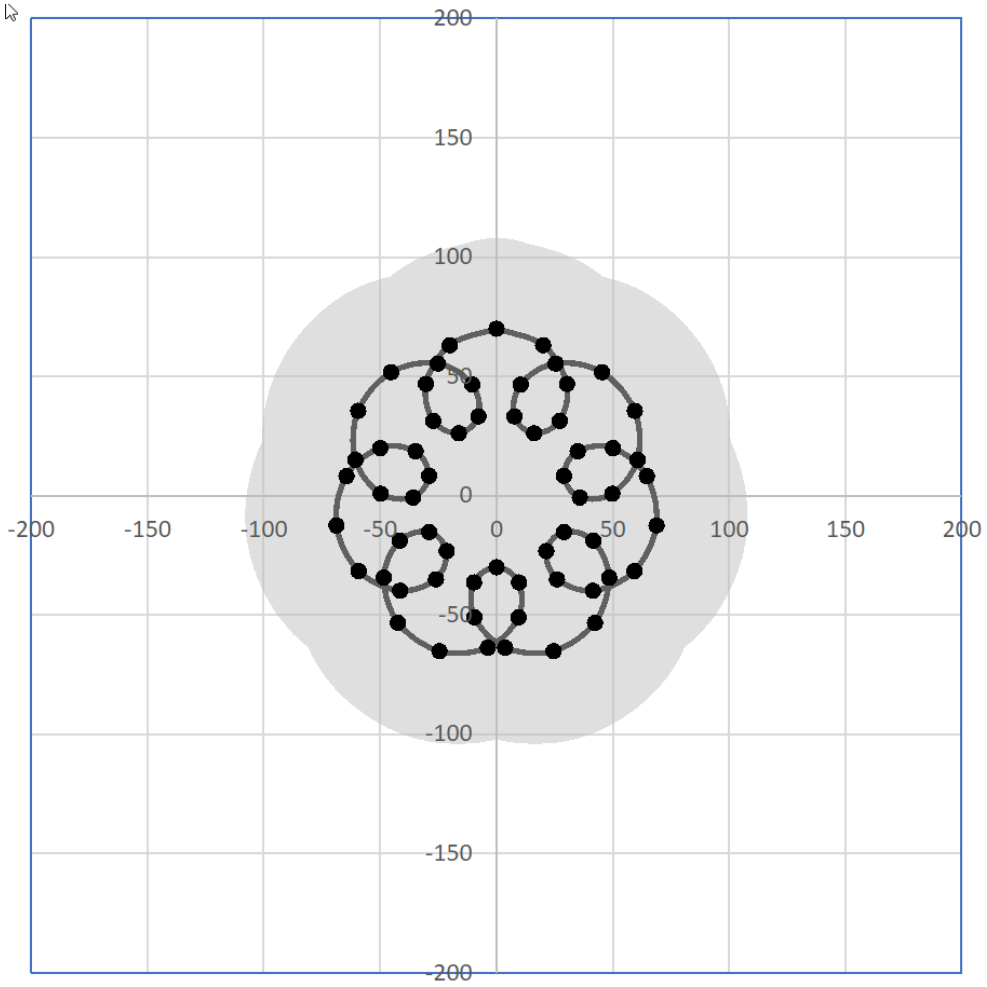

Figure 6. Example plot of calculated discrete position points used to program the robot. Axis values in millimeters; grey marks the area covered by the used debridement product.

Determination of real-time debridement forces

To investigate contact forces applied during debridement processes, physicians with professional experience in wound care were included in an exemplary analysis. They were given the task to imitate real mechanical wound debridement processes on a scale, either directly via *DebriTrack* or, in the high weight range, on a common scale. The measurements revealed a wide load range. Low forces are preferred in order to perform the treatment as gently and painless as possible. These can be sufficient for the removal of exudate or fibrin. High loads, with peak values in the double-digit kilogram range, become necessary for effective debridement of burns and necroses. To cover necessary debridement forces for the entire spectrum of wounds, the system was designed for a load range between 0.75 kg and 19 kg.

Replication of real wound fluids and coatings

Simulations of exudate, fibrin coatings, burns and necroses, representing the physical behavior of real wounds, were developed in our laboratories. Their comparability with reality in terms of physical properties was examined by experienced clinicians.

Various formulations were developed to simulate different wound exudate phases of infection and healing, ranging from serous to viscous. To reproduce serous exudates, a water-based 10 % egg white powder protein solution was developed. For the simulation of transitional exudate forms, the viscosity of the solution can be increased in stages by raising protein content (from 20 % egg white powder to 24 % egg white powder plus 10 % milk powder). To achieve an even more viscous stage, fatty additives (2 %), like beef fat powder, can be added. Furthermore, fibrinous exudate is simulated by adding solids, such as lipo-particles or wheat bran (2.4 %).

Fibrin coatings can be simulated by using gelatin (for jelly-like properties) and collagen (for grip to the surface and viscosity) in different proportions (3:4, 1:1, or 4:3), leading to diverse physical

properties. Additives, such as transglutaminase (for structural binding), can be added to gelatin and collagen (1:1:2) for adjustment of the physical properties. Ingredients are dissolved in water (gelatin to water 1:4, collagen to water 3:4, transglutaminase to water 2.5:10) and mixed on a heat plate at 50 °C. For all described mixtures, Ringer's solution can be used as an alternative to water. Duration of drying time determines the hardness of coatings.

Burns and necroses can be simulated by a mixture of paraffin (for waxy structure) and cellulose (to loosen up the structure). The proportions of the two components determine the properties (4.3:1; 5.4:1, or 7.2:1). To facilitate visualization and presentation for documentation purposes, all formulations can be dyed red using a colorant (Ponceau 4R, 0.05%).

Application of the semi-automated robotic system

To verify our test system in its entirety, test series were performed (Fig S1 – S4). A selection of velocities and contact forces were applied with a hypocycloid movement (Fig 6) based on clinical records (Fig 4). A commercial fiber debridement product was used for debriding the artificial wounds. Efficacy of wound debridement and product uptake was analyzed.

The test execution worked correctly from the technical point of view. Data analysis was performed via weight measurements of simulated wounds and debridement products before and after the simulated debridement process (Fig S1 – S4) using statistics software R (R Core Team/AT, Version 3.6.2) [18, 19].

Adjusting parameters such as contact force (Fig S1 – S2) or velocity (Fig S3 – S4) resulted in significantly different data. Obtained data showed a low coefficient of variation as well as a low standard deviation. Images taken before and after debridement support the data visually. Images of the individual debridement steps (data not shown here) as well as overview images were taken (Fig 7). Results are consistent within multiple test series (data not shown here), which proves

reproducibility. Electronic notebook platform was not used. Data are currently not publicly available or accessible.

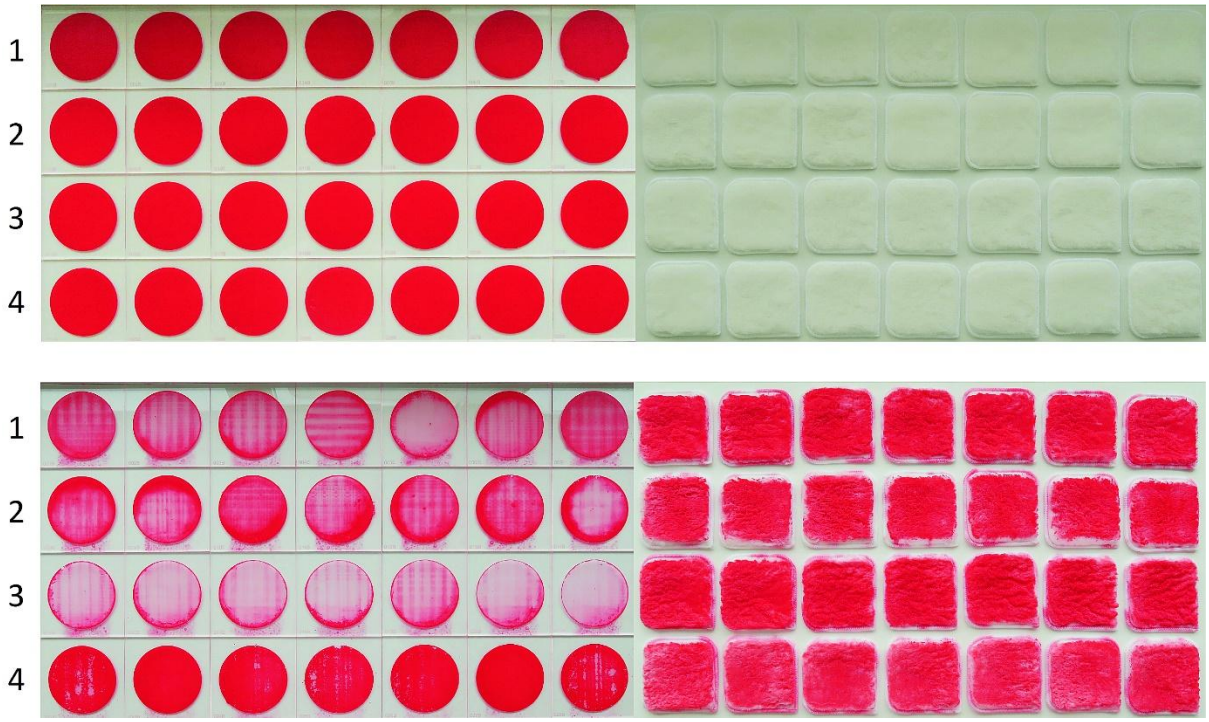

Figure 7. Visualized results (overview image): wound plates with serous exudate and fiber debridement products before (above images) and after (bottom images) debridement procedure. Analyzed under different *DebriSim* settings; 1.) 2,5 kg, 20 mm/s, hypocycloid movement, 1 cycle; 2.) 0,75 kg, 20 mm/s, hypocycloid movement, 1 cycle; 3.) 5 kg, 20 mm/s, hypocycloid movement, 1 cycle; 4.) 2,5 kg, 160 mm/s, hypocycloid movement, 1 cycle.

Discussion

The presented system enables a detailed analysis of mechanical debridement procedures and wound debridement products in a semi-automated, clinic-oriented, and reproducible way. Patients of all ages with both chronic and acute wounds can benefit from the enhanced wound debridement strategies provided by our approach. Optimized wound care leads to a higher quality of life by addressing problems such as intense pain, malodor, decreased mobility, long treatment times, and increased mortality. In addition, optimized wound management saves resources by reducing time-consuming, costly, and waste generating treatment steps.

It is estimated that more than 13 million people in the world are affected by chronic wounds each year [20]. Around half of chronic wounds treated with standard procedures fail to heal within one year [21]. Due to population ageing, the total number of affected people will increase further. It is forecasted that 20–60 million people worldwide will suffer from chronic skin wounds by 2026 [22]. According to a market analysis, the global wound debridement market size is anticipated to reach USD 6.97 billion by 2025 [23]. Our test system can be used to develop and promote high-performance products that are essential to cover the future demand of wound treatment. With our setup technologies can be evaluated objectively and products on the marked become comparable.

Combining "*DebriTrack*" (Fig 2, Mov S1) and "*DebriSim*" (Fig 3, Mov S2) allows for the first time to record real debridement patterns (e.g., Fig 4) and to teach the robot these sequences. Artificial wounds that simulate various wound characteristics complete our test system. Moreover, wound surrounding skin, including its physical properties, can be simulated as well (data not shown here). Wound models described in the past often exclusively simulate a healthy surface [24] or are not sufficiently realistic [25, 26]. Biological wound models, e.g., based on pig skin [15], have a short shelf life,

are restricted to guidelines, and are subjected to natural variations that may result in low data reproducibility. We showed that the adjustment of parameters, such as contact force (Fig S1 – S2) or velocity (Fig S3 – S4), on *DebriSim* results in significant changes in debridement success. Low variation coefficient as well as low standard deviation of our obtained data indicate the reliability of our system, which allows reproducible tests to be performed.

Previous technical test systems were limited to simple movements and low loads [6, 7, 9, 10, 11, 12, 13]. However, contact forces during real clinical debridement processes can reach high values. Also, the medical staff applies different and individually modified patterns for adequate wound debridement procedures (e.g., Fig 4; further data not shown here). Due to its flexible parameter settings, our robotic system can reflect the full range of realistic debridement parameters. Besides the possibility of procedure analysis in clinics, the robot also enables an assessment of wound treatment procedures recommended in training literature [27, 28]. Obtained data supports the user to perform wound debridement in an advanced manner, tailored to individual wound situations. Wound management trainings based on our test system could be offered.

The closed loop between real-time applications and *in-vitro* analysis is the core element of our test system. It can be transferred to various application areas, such as tests of abrasion, adhesion, disinfection, peeling and fiber release. Moreover, cleaning proofs or analysis to prevent smearing of infectious wound fluids could be conducted.

Our test system has the potential to become an internationally renowned test standard, enabling reproducible multi-site investigations in a very short time. Expanded testing capabilities support scientific progress that may lead to new approaches revolutionizing modern wound debridement.

Moreover, our robotic test system has the potential to replace a substantial part of extensive and expensive *in-vivo* studies, such as tests of product performance on humans [29] or animals. Animal testing is associated with high suffering and should be prevented wherever possible. It is important to note that for some scientific questions an *in-vitro* approach is even more suitable than an *in-vivo* test. This fact may lead to a paradigm shift in medical device testing [30].

In the future, real debridement application data can be continuously loaded into the robot's memory. To support and relieve medical staff, the robotic system could be further developed to perform optimized debridement procedures directly on the patient. This includes wound analysis by a specifically developed scanning system, followed by a debridement program tailored to the evaluated wound situation. Our models and test procedures will be continuously optimized, resulting in a circular improvement process (Fig 1). The constantly growing spectrum of analysis options for wound debridement products and processes enables continuous optimization of debridement procedures. In its entirety, our developed test system strongly supports the overall goal of clinical benefit.

Funding Statement

This work has been supported by ACMIT – Austrian Center for Medical Innovation and Technology, which is funded within the scope of the COMET – Competence Centers for Excellent Technologies program and by the federal government (BMDW and BMK), the federal government of Lower Austria and the Standortagentur Tirol.

References

1. Strohal R, Apelqvist J, Dissemond J, et al. EWMA Document: Debridement. J Wound Care 2013; 22(1):1–52.

2. Zhao R, Liang H, Clarke E, et al. Inflammation in Chronic Wounds. Int J Mol Sci 2016; 17(12):2085; doi: 10.3390/ijms17122085.

3. Nicks BA, Ayello EA, Woo K, et al. Acute wound management: revisiting the approach to assessment, irrigation, and closure considerations. Int J Emerg Med 2010; 3(4):399–407; doi: 10.1007/s12245-010-0217-5.

4. Schwegman D, Gelly HB. A practical guide to establishing a wound care formulary in your clinic. Today's Wound Clinic 2019; 13(6):10–12.

5. Gillespie BM, Chaboyer W, St John W, et al. Health professionals' decision-making in wound management: a grounded theory. J Adv Nurs 2015; 71(6):1238–1248; doi: 10.1111/jan.12598.

6. Wiegand C, Reddersen K, Abel M, et al. In vitro evaluation of the debridement performance of a new debrider compared to conventional cotton gauze. XI. Congresso Nazionale AIUC, Rimini; 2012. Available from: https://www.lohmann-rauscher.com/fileadmin/publications/Wiegand__Reddersen_et_al._26.09.2012_-_In_vitro_evaluation.pdf [Last accessed: 01/17/2023].

7. Reddersen K, Wiegand C, Abel M, et al. Determination of the reduction of biofilm in vitro during wound cleansing using a monofilament debrider and conventional cotton gauze. EWMA, Madrid; 2014. Available from: https://www.lohmann-rauscher.com/fileadmin/publications/Wiegand__Reddersen_et_al._14.05.2014_-_Determination_of_the_reduction.pdf [Last accessed: 01/23/2023].

8. Wiegand C, Reddersen K, Abel M, et al. Determination of the reduction of biofilm in vitro during wound cleansing using a monofilament debrider, a cleansing system with poloxamer, and conventional cotton gauze. Wounds UK Annual Conference, Harrogate; 2014. Available from: https://debrisoft.com/wp-content/uploads/2018/03/Wiegand-Reddersen-et-al.-10.11.2014-Determination-of-the-reduction.pdf [Last accessed: 01/23/2023].

9. Wiegand C, Reddersen K, Hipler UC, et al. In vitro evaluation of the cleansing effect of a monofilament fiber debridement pad compared to gauze swabs. Skin Pharmacol Physiol 2016; 29(6):318–323; doi: 10.1159/000454720.

10. Wiegand C, Reddersen K, Abel M, et al. Evaluation of the cleansing capacity of a monofilament debrider device compared to conventional cosmetic pads in a sebum model. Wounds UK Annual Conference, Harrogate; 2017. Available from: https://www.lohmann-rauscher.com/fileadmin/publications/Wiegand__Reddersen_et_al._13.11.2017_-_Evaluation_of_the_cleansing_capacity.pdf [Last accessed: 01/17/2023].

11. Wilkinson HN, McBain AJ, Stephenson C, et al. Comparing the effectiveness of polymer debriding devices using a porcine wound biofilm model. Adv Wound Care Adv Wound Care (New Rochelle) 2016; 5(11):457–485; doi: 10.1089/wound.2015.0683.

12. Gafford J, Ranzani T, Russi S, et al. Towards medical devices with integrated mechanisms, sensors and actuators via printed-circuit MEMS. J Med Device 2017; 11(1):011007-1–011007-12; doi: 10.1115/1.4035375.

13. Igwebuike H, Hoeier Nielsen K. Wound care device for debriding wounds. WO 2019/057256 A1; 2019.

14. Karnam MK, Asokan T. Association for Computing Machinery. Design and analysis of a robotic system for acute wound cleaning. AIR '13, Pune; 2013; pp. 1–6. doi: 10.1145/2506095.2506135.

15. Schoeb DS, Klodmann J, Schlager D, et al. Robotic waterjet wound debridement – Workflow adaption for clinical application and systematic evaluation of a novel technology. PLOS ONE 2018; 13(9): e0204315; doi: 10.1371/journal.pone.0204315.

16. Schlenk C, Schwier A, Heiss M, et al. Design of a robotic instrument for minimally invasive waterjet surgery. ISMR, Atlanta; 2019. Available from: https://elib.dlr.de/141614/1/ISMR2019_Waterjet_Accepted_Version.pdf [Last accessed: 01/17/2023].

17. Liu Yan. Intelligent examining, medicine applying and sampling integrated device for department of gynaecology and obstetrics. CN105726067B; 2018.

18. R Core Team. R Foundation for Statistical Computing, Vienna, Austria. R: A language and enviroment for statistical computing; 2019. Available from: http://www.R-project.org/ [Last accessed 01/24/2022].

19. Wickham H, Averick M, Bryan J, et al. Welcome to the tidyverse. J Open Source Softw 2019; 4(43):1686; doi: 10.21105/joss.01686.

20. Chakraborty C, Gupta B, Ghosh SK, et al. Mobile metadata assisted community database of chronic wound images. Wound Medicine 2014; 6(24–42); doi: 10.1016/j.wndm.2014.09.002.

21. Guest JF, Fuller GW, Vowden P. Cohort study evaluating the burden of wounds to the UK's National Health Service in 2017/2018: update from 2012/2013. BMJ Open 2020; 10:e045253; doi: 10.1136/bmjopen-2020-045253.

22. MedMarket Diligence. Worldwide Wound Management, Forecast to 2026: Established and Emerging Products, Technologies and Markets in the Americas, Europe, Asia/Pacific and Rest of World; 2018.

23. Grand View Research, Inc. Wound Debridement Market Analysis Report By Product (Gels, Ointments & Creams), By Method, By Wound Type (Diabetic Foot, Pressure Ulcers), By End Use, And Segment Forecasts, 2018 – 2025; 2018. https://www.grandviewresearch.com/industry-analysis/wound-debridement-market [Last accessed 03/10/2021].

24. Jussila J, Leppäniemi A, Paronen M, et al. Ballistic skin simulant. Forensic Sci Int 2005; 150(1):63–71; doi: 10.1016/j.forsciint.2004.06.039.

25. Bahls T, Fröhlich FA, Hellings A, et al. Extending the capability of using a waterjet in surgical interventions by the use of robotics. IEEE Trans Biomed Eng 2017; 64(2):284–294; doi: 10.1109/TBME.2016.2553720.

26. Kehoe B, Kahn G, Mahler J, et al. IEEE Robotics and Automation Society. Autonomous multilateral debridement with the Raven surgical robot. ICRA, Hong Kong; 2014; pp. 1432–1439; doi: 10.1109/ICRA.2014.6907040.

27. Trott AT (ed). Wounds and lacerations: emergency care and closure, 4th ed. In: wound cleansing and irrigation. W.B. Saunders Ltd.: Philadelphia; 2012; pp. 73–81; doi: 10.1016/B978-0-323-07418-6.00007-1.

28. U.S. Army Medical Department Center and School. Sterile procedures, 100th ed. Subcourse MD0540. In: lesson 4. procedures used in wound care. Texas; 2017. Available from: http://nursing411.org/Army/MD0540.pdf [Last accessed: 01/24/2023].

29. Iblasi AKS. Comparing the clinical performance of two selected mechanical wound debridement products in sloughy pressure ulcers. Wounds Middle East 2018; 5(1):11–16.

30. Kerecman Myers D, Goldberg AM, Poth A, et al. From in vivo to in vitro: The medical device testing paradigm shift. ALTEX 2017; 34(4):479–500; doi: 10.14573/altex.1608081.

Figure Legends

Figure 1. Innovation process. The semi-automatic robot system comprises a repeating input-output process. Inputs are generated by real-time tracking of debridement procedures simulated by wound care professionals. The recorded data are technically processed to feed the debridement parameters into the robot, which reproduces them. After execution of the debridement process by the robot on simulated wounds, the obtained output is evaluated. Clinical wound debridement processes can be optimized based on the acquired knowledge.

Figure 2. *DebriTrack*. The device includes a force sensing platform (not shown here), a test surface depicting a virtual wound and modified debridement test products, equipped with a conductive mesh (front and back side shown). The force sensing platform and the tablet PC are connected via USB.

Figure 3. *DebriSim*. Schematic representation of the robot construction with inserted artificial wounds and an attached test sample on the gripper.

Figure 4. Sample of a hypocycloid movement pattern from a real-time recording created by a medical wound manager. Red circle = wound area, black line = recorded track (center of the debridement product served as contact area)

Figure 5. Graphical illustration for the generation of a hypocycloid for point P.

Figure 6. Example plot of calculated discrete position points used to program the robot. Axis values in millimeters; grey marks the area covered by the used debridement product.

Figure 7. Visualized results (overview image): wound plates with serous exudate and fiber debridement products before (above images) and after (bottom images) debridement procedure. Analyzed under different

DebriSim settings; 1.) 2,5 kg, 20 mm/s, hypocycloid movement, 1 cycle; 2.) 0,75 kg, 20 mm/s, hypocycloid movement, 1 cycle; 3.) 5 kg, 20 mm/s, hypocycloid movement, 1 cycle; 4.) 2,5 kg, 160 mm/s, hypocycloid movement, 1 cycle.

Figure S1. Wound debridement efficacy of fiber debridement products under different weight settings. Serous exudate simulation on large wound plates (base plate = 150 x 150 mm, circular diameter of simulated wound area = 120 mm) was used to mimic the wound situation (environmental conditions: 21.5 °C, 42,8 % RH). For data analysis, wound plates were weighted before and after simulated debridement procedure with *DebriSim*. Parameter settings were either 0.75 kg, 2.5 kg or 5 kg paired with 20 mm/s, applying a hypocycloid movement without repetition. Statistical analysis was performed using R (version 3.6.2) [18, 19]. F-Test was used to analyze the equality of the variances between the groups together with t-test to compare the means of the groups. P values < 0,05 were considered significant (*), < 0,05 very significant (**) and < 0,05 highly significant (***). All data are presented as mean ± standard deviation.

Figure S2. Product uptake of fiber debridement products under different weight settings. Serous exudate simulation on large wound plates (base plate = 150 x 150 mm, circular diameter of simulated wound area = 120 mm) was used to mimic the wound situation (environmental conditions: 21.5 °C, 42,8 % RH). For data analysis, products were weighted before and after simulated debridement procedure with *DebriSim*. Parameter settings were either 0.75 kg, 2.5 kg or 5 kg paired with 20 mm/s, applying a hypocycloid movement without repetition. Statistical analysis was performed using R (version 3.6.2) [18, 19]. F-Test was used to analyze the equality of the variances between the groups together with t-test to compare the means of the groups. P values < 0,05 were considered significant (*), < 0,05 very significant (**) and < 0,05 highly significant (***). All data are presented as mean ± standard deviation.

Figure S3. Wound debridement efficacy of fiber debridement products under different velocity settings. Serous exudate simulation on large wound plates (base plate = 150 x 150 mm, circular diameter of simulated wound area = 120 mm) was used to mimic the wound situation (environmental conditions: 21.5 °C, 42,8 % RH). For data analysis, wound plates were weighted before and after simulated debridement procedure with *DebriSim*. Parameter settings were either 20 mm/s or 160 mm/s paired with 2.5 kg, applying a hypocycloid movement without repetition. Statistical analysis was performed using R (version 3.6.2) [18, 19]. F-Test was used to analyze the equality of the variances between the groups together with t-test to compare the means of the groups. P values < 0,05 were considered significant (*), < 0,05 very significant (**) and < 0,05 highly significant (***). All data are presented as mean ± standard deviation.

Figure S4. Product uptake of fiber debridement products under different velocity settings. Serous exudate simulation on large wound plates (base plate = 150 x 150 mm, circular diameter of simulated wound area = 120 mm) was used to mimic the wound situation (environmental conditions: 21.5 °C, 42,8 % RH). For data analysis, products were weighted before and after simulated debridement procedure with *DebriSim*. Parameter settings were either 20 mm/s or 160 mm/s paired with 2.5 kg, applying a hypocycloid movement without repetition. Statistical analysis was performed using R (version 3.6.2) [18, 19]. F-Test was used to analyze the equality of the variances between the groups together with t-test to compare the means of the groups. P values < 0,05 were considered significant (*), < 0,05 very significant (**) and < 0,05 highly significant (***). All data are presented as mean ± standard deviation.